

Data-based fuel-economy optimization of connected automated trucks in traffic

Chaozhe R. He, Jin I. Ge, and Gábor Orosz

Abstract—In this paper we perform fuel-economy optimization for a connected automated truck that utilizes motion information from multiple vehicles ahead via vehicle-to-vehicle (V2V) communication. Position and velocity data collected from a chain of human-driven vehicles is utilized to design a connected cruise controller that can respond to traffic perturbations while maximizing energy efficiency. The results are compared to those obtained using a high-fidelity truck model and the robustness of the design is validated on multiple data sets. It is shown that optimally utilizing V2V connectivity may lead to 4%-13% fuel economy improvements compared to the best non-connected design.

I. INTRODUCTION

Heavy-duty vehicles account for a large percentage of fuel consumption in road transportation systems [1]. Improving their fuel economy would benefit the trucking industry while carrying large societal benefits. To tackle this problem one may use geo-location information to determine optimal speed profiles that maximize the fuel economy [2], [3]. However, these speed profiles may be difficult to follow by trucks in real traffic, when they need to respond to the speed perturbations propagating from human-driven vehicles ahead.

Automated trucks may respond better to the traffic perturbations and achieve better fuel economy [4]. Yet the improvements may be limited due to the fact that on-board sensors can only obtain information within its line of sight, and thus the controller for a sensor-based automated truck seldom considers motion information from more than one vehicle ahead. To further improve the fuel economy, one can use vehicle-to-vehicle (V2V) communication to monitor the motion of multiple vehicles ahead, and utilize beyond-line-of-sight information [5]–[8]. While numerical optimization methods can be used to achieve better fuel economy when the motion of the preceding vehicles can be accurately predicted [9], [10], the performance of such controllers may not be ideal in real traffic [11].

In this paper, we utilize traffic data collected from a chain of human-driven vehicles and design connected cruise controllers that optimize fuel economy for heavy-duty vehicles. We establish a design method that can ensure energy-efficient responses to the traffic perturbations and demonstrate its

impacts on fuel economy using high-fidelity TruckSim simulations. We show the robustness of the design by testing the controller on multiple different data sets.

II. TRAFFIC DATA FOR CONNECTED AUTOMATED TRUCK DESIGN

In this section, we present the speed profiles of human-driven vehicles and analyze the characteristics of the speed perturbations from a series of on-road experiments, in order to design a connected automated truck that will perform well among human-driven vehicles.

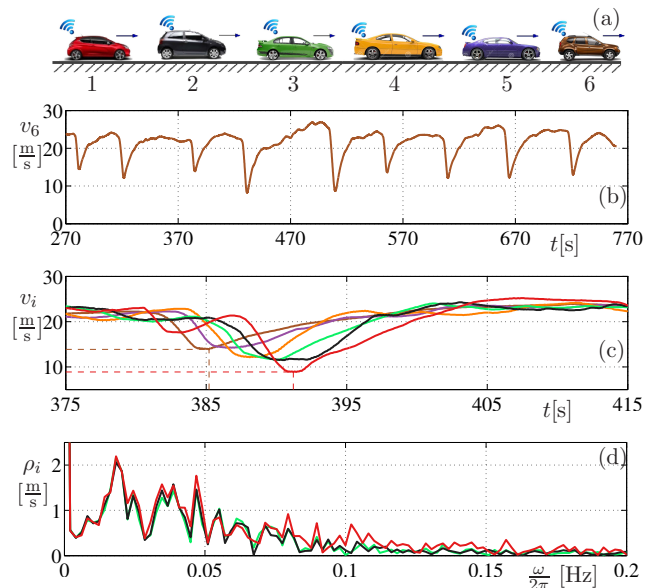


Fig. 1: (a) Six human-driven vehicles traveling on a one-lane road with no elevation. (b) The speed profile of the head vehicle 6. (c) Speed profiles of the six vehicles during one braking event. (d) The amplitude spectra of velocity profiles of vehicles 1, 2, 3 during the experiment.

We recorded the speed and position data of six consecutive human-driven vehicles on a segment of flat road that has one lane in each direction; see Fig. 1(a). Vehicle 6 led this vehicle chain with a series of mild braking events, while its average velocity was about 20 [m/s]; see Fig. 1(b). Such mild velocity variations have been observed frequently in urban and highway traffic, especially when traffic jams start to appear [12]. In Fig. 1(c), we show the velocity profiles of the six vehicles during one mild braking event. As the perturbation cascades along the vehicle chain, the minimum speed decreases from around 14 [m/s] for vehicle 6 (brown) for about 9 [m/s] on vehicle 1 (red). Such a

This work was supported by the University of Michigan Mobility Transformation Center

Chaozhe R. He and Gábor Orosz are with the Department of Mechanical Engineering, University of Michigan, Ann Arbor, MI 48109 {hchaozhe, orosz}@umich.edu

Jin I. Ge is with the Department of Computing and Mathematical Sciences, California Institute of Technology, Pasadena, CA 91125 jge@caltech.edu

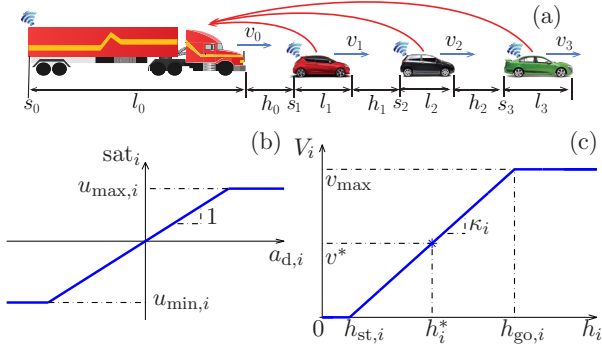


Fig. 2: (a) Layout of the connected vehicle system with a heavy-duty vehicle at the tail controlled by a connected cruise control algorithm. Each preceding vehicle is reacting to motion of the vehicle immediately ahead while the truck utilizes V2V information about 3 vehicles ahead. (b) The saturation function in (1). (c) The range policy function (4).

phenomenon is an example of string instability in human-dominated traffic, where human drivers are generally unable to suppress the speed perturbations propagating through the traffic flow [6]. These speed perturbations would force a truck to deviate from fine-tuned driving strategies that may guarantee good fuel economy under ideal driving cycles. Therefore, to maintain desirable fuel economy in real traffic, longitudinal controllers for trucks should be designed with consideration of the traffic perturbations.

To extract the characteristics of these speed perturbations, we perform fast Fourier transform and present the amplitude spectra for vehicles 1, 2, 3 in Fig. 1(d). We observe that the speed perturbations are mainly low-frequency oscillations. While the frequency components of speed perturbations may be different for different road segments, using V2V communication we may collect motion information from multiple vehicles ahead and obtain the amplitude spectra of speed perturbations in real time. In this way, the connected automated truck is able to target specific kinds of speed perturbations and actively mitigate their influence to benefit its fuel economy.

III. CONNECTED CRUISE CONTROL DESIGN

In this section, we design the longitudinal control for a connected automated truck that utilizes V2V information from multiple human-driven vehicle ahead; see Fig. 4(a). We first model the human driving behavior as a feedback controller, then we propose a class of connected cruise controllers that include direct feedback on motion signals from more than one vehicle ahead. By tuning the corresponding feedback gains, a connected automated truck is able to respond to speed perturbations while optimizing its fuel economy.

We describe the longitudinal motion of both human-driven vehicles and connected automated trucks with

$$\begin{aligned} \dot{s}_i(t) &= v_i(t), \\ \dot{v}_i(t) &= -f_i(v_i(t)) + \tilde{f}_i(v_i(t - \zeta_i)) + \text{sat}_i(a_{d,i}(t - \zeta_i)), \end{aligned} \quad (1)$$

where the dots denote differentiation with respect to time t , s_i denotes the position of the rear bumper of vehicle i , v_i denotes its velocity, and ζ_i is the throttle/brake response time that can also be approximated by a first order lag [6], [10]; see Fig. 2(a). The term $f_i(v_i)$ collects the physical effects like air resistance and rolling resistance, while $\tilde{f}_i(v_i)$ denotes the compensation for these physical effects that is often implemented in the lower-level controller. Finally, $a_{d,i}$ denotes the higher-level acceleration command that we focus on designing while exploiting V2V information to optimize fuel economy. The saturation function $\text{sat}_i(\cdot)$ limits the commanded acceleration between $u_{\min,i}$ and $u_{\max,i}$ based on the engine and braking power limits; see Fig. 2(b).

A. Human acceleration control behavior

We describe the acceleration control command given by the human driver for vehicle i as

$$\begin{aligned} a_{d,i}(t) &= \alpha_{h,i} \left(V_i(s_{i+1}(t - \xi_{h,i}) - s_i(t - \xi_{h,i}) - l_i) \right. \\ &\quad \left. - v_i(t - \xi_{h,i}) \right) \\ &\quad + \beta_{h,i} (v_{i+1}(t - \xi_{h,i}) - v_i(t - \xi_{h,i})). \end{aligned} \quad (2)$$

Here, $\alpha_{h,i}$ and $\beta_{h,i}$ are the control gains used by the human driver, while the time delay $\xi_{h,i}$ is the driver reaction time, and $i = 1, \dots, n - 1$. In (2), the bumper-to-bumper distance

$$h_i = s_{i+1} - s_i - l_i \quad (3)$$

is referred to as the headway of vehicle i , where l_i denotes the length of vehicle i . The range policy function $V_i(h_i)$ describes the desired velocity of vehicle i as a function of its headway. In this paper, we use

$$V_i(h_i) = \begin{cases} 0 & \text{if } h_i \leq h_{\text{st},i}, \\ \kappa_i(h_i - h_{\text{st},i}) & \text{if } h_{\text{st},i} < h_i < h_{\text{go},i}, \\ v_{\max} & \text{if } h_i \geq h_{\text{go},i}, \end{cases} \quad (4)$$

as shown in Fig. 2(c). For a small headway ($h_i < h_{\text{st},i}$), the vehicle intends to stop; for a large headway ($h_i > h_{\text{go},i}$), it intends to travel with the speed limit v_{\max} ; between $h_{\text{st},i}$ and $h_{\text{go},i}$ the desired velocity increases linearly, with the gradient $\kappa_i = v_{\max}/(h_{\text{go},i} - h_{\text{st},i})$. Note that when $h_{\text{st},i} = 0$, (4) corresponds to the constant time headway $1/\kappa_i$. For more discussions on the range policy function, see [6].

B. Connected cruise control

Here we present a framework for connected cruise control design that explicitly uses the motion information received from multiple vehicles ahead. In particular, we consider the control law

$$\begin{aligned} a_{d,0}(t) &= \alpha \left(V_0(s_1(t - \xi_1) - s_0(t - \xi_1) - l_0) - v_0(t - \xi_1) \right) \\ &\quad + \sum_{i=1}^n \beta_i (v_i(t - \xi_i) - v_0(t - \xi_i)). \end{aligned} \quad (5)$$

Here α and β_i are the feedback gains to be tuned for a better fuel economy. The range policy function $V_0(\cdot)$ is given by (4) but its gradient κ_0 and distances $h_{\text{st},0}$, $h_{\text{go},0}$ may differ from those used by human drivers. Also, ξ_i represents the

delay of information from vehicle i due to signal sampling and communication intermittency. Note that $\sigma_i = \xi_i + \zeta_0$ gives the total delay in the control loop. In this paper, we set $\sigma_i = \sigma$ for $i = 1, \dots, n$ for simplicity.

Without V2V communication, an automated truck is only able to include feedback terms using motion information from its immediate predecessor, vehicle 1. In this case, $n = 1$ for the sum in (5). By including speed information from vehicle $i \geq 2$, that is usually beyond the perception range of human eyes or on-board sensors, we expect to gain more improvement in the fuel economy of the connected automated truck.

IV. OPTIMAL CONNECTED CRUISE CONTROL FOR TRUCKS AMONG HUMAN-DRIVEN VEHICLES

In this section, we first present an analytical method to quantify the energy efficiency of the connected cruise controller (5) based on experimental data. Then we use this method to find the most energy efficient feedback gains. Finally, a high-fidelity simulation platform is used to relate energy efficiency to fuel efficiency.

A. Data-based optimization for energy efficiency

Here we present a method to relate the feedback gains α and β_i in the controller (5) with the energy efficiency of the connected automated truck while considering the Fourier spectrum of speed perturbations on road.

We consider the scenario where a connected automated truck drives behind a chain of human-driven vehicles on a flat road with zero grade, as shown in Fig. 2(a). The motion of each vehicle fluctuates around an equilibrium

$$s_i^*(t) = v^*t + \bar{s}_i, \quad v_i(t) \equiv v^*, \quad (6)$$

where vehicles travel with the same constant speed while keeping constant distances

$$h_i^* = \bar{s}_{i+1} - \bar{s}_i - l_i, \quad v^* = V_i(h_i^*) \quad (7)$$

for $i = 0, \dots, n$; see Fig. 2(a). We remark that v^* can be obtained from traffic data as Fourier coefficient for zero frequency. That is, $\rho_i(0) = v^*$ for $i = 1, \dots, n$; see Fig. 1(d) where $v^* \approx 21.5$ [m/s]. We define the perturbations $\tilde{s}_i = s_i - s_i^*$, $\tilde{v}_i = v_i - v^*$, and assume the influence of the physical effects $f_i(v_i)$ can be negated by $\tilde{f}_i(v_i)$. Then, around the uniform flow (6), the linearized dynamics of the connected vehicle system (1,2,5) becomes

$$\begin{aligned} \dot{\tilde{s}}_0(t) &= \tilde{v}_0, \\ \dot{\tilde{v}}_0(t) &= \alpha \left(\kappa_0 (\tilde{s}_1(t - \sigma) - \tilde{s}_0(t - \sigma)) - \tilde{v}_0(t - \sigma) \right) \\ &\quad + \sum_{k=1}^n \beta_k (\tilde{v}_k(t - \sigma) - \tilde{v}_0(t - \sigma)), \\ \dot{\tilde{s}}_i(t) &= \tilde{v}_i(t), \\ \dot{\tilde{v}}_i(t) &= \alpha_{h,i} \left(\kappa_i (\tilde{s}_{i+1}(t - \tau_i) - \tilde{s}_i(t - \tau_i)) - \tilde{v}_i(t - \tau_i) \right) \\ &\quad + \beta_{h,i} (\tilde{v}_{i+1}(t - \tau_i) - \tilde{v}_i(t - \tau_i)), \end{aligned} \quad (8)$$

for $i = 1, \dots, n-1$ where $\tau_i = \xi_{h,i} + \zeta_i$ is the lumped time delay in human-driven vehicles.

We approximate the velocity perturbation \tilde{v}_n of vehicle n using the m leading frequency components

$$\tilde{v}_n(t) = \sum_{j=1}^m \rho_{n,j} \sin(\omega_j t + \phi_{n,j}), \quad (9)$$

where the frequency is discretized as $\omega_j = j\Delta\omega$ with $\Delta\omega = 0.002$ [Hz], $\rho_{n,j} = \rho_n(\omega_j)$ is the amplitude of speed oscillation at frequency ω_j , and $\phi_{n,j} = \phi_n(\omega_j)$ is the corresponding phase angle; see Fig. 1(d). Based on the linearized dynamics of connected vehicle system (8), the steady-state oscillation of the connected automated truck can be expressed as

$$\tilde{v}_0(t) = \sum_{j=1}^m \rho_{n,j} |\Gamma_n(i\omega_j; \mathbf{p}_n)| \sin(\omega_j t + \phi_{n,j} + \angle \Gamma_n(i\omega_j; \mathbf{p}_n)), \quad (10)$$

where we utilize the head-to-tail transfer function

$$\Gamma_n(\lambda; \mathbf{p}_n) = \frac{\lambda \sum_{i=1}^n \beta_i \prod_{k=i}^{n-1} H_k(\lambda) + \alpha \kappa_0 \prod_{k=1}^{n-1} H_k(\lambda)}{\lambda^2 e^{\lambda\sigma} + \lambda \left(\alpha + \sum_{i=1}^n \beta_i \right) + \alpha \kappa_0}, \quad (11)$$

with $\mathbf{p}_n = [\alpha, \kappa, \beta_1, \dots, \beta_n]$ containing the design parameters and

$$H_k(\lambda) = \frac{\beta_{h,k} \lambda + \alpha_{h,k} \kappa_k}{\lambda^2 e^{\lambda\tau_k} + \lambda(\alpha_{h,k} + \beta_{h,k}) + \alpha_{h,k} \kappa_k}, \quad (12)$$

for $k = 1, \dots, n-1$ describe the human drivers; see [13].

We define the work per unit mass carried out to accelerate the vehicle during the time interval $[t_0, t_f]$ as

$$W = \int_{t_0}^{t_f} v_0(t) g(\dot{v}_0(t) + f(v_0(t))) dt, \quad (13)$$

with nonlinear function $g(x) = \max(0, x)$. It can be shown that finding the parameter vector \mathbf{p}_n that minimizes W can be approximated by minimizing the objective function

$$J_n(\mathbf{p}_n) = \sqrt{\sum_{j=1}^m \omega_j^2 \rho_{n,j}^2 |\Gamma_n(i\omega_j; \mathbf{p}_n)|^2}. \quad (14)$$

Thus, by computing the level sets of (14) the connected automated truck is able to relate the values of the control gains in (5) with its energy efficiency (at the linear level).

B. Fuel consumption optimization by high-fidelity simulation

In order to take into account realistic vehicle and powertrain dynamics of the connected automated truck, we set up a high-fidelity truck model in TruckSim. This allows us to estimate the fuel consumption and relate it to the energy efficiency defined in the previous section.

Fig. 3 shows the simulation platform for the connected automated truck in MATLAB/Simulink, containing the TruckSim module that uses specifications of a Navistar Prostar truck [14]. We implement the higher-level connected

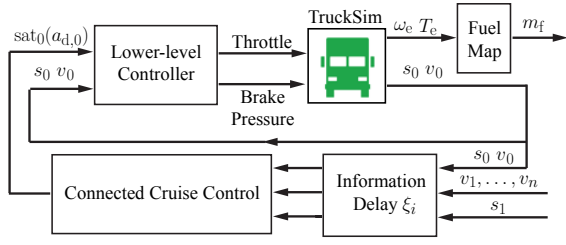


Fig. 3: Conceptual block diagram of the TruckSim and MATLAB/Simulink co-simulation for fuel consumption estimation.

cruise controller (5) and a lower-level controller with the compensation function

$$\tilde{f}_0(v_0) = \frac{1}{m_{\text{eff}}}(\gamma mg + \eta v_0^2), \quad (15)$$

where the effective mass $m_{\text{eff}} = m + I/R^2$ includes the mass of the vehicle m , the moment of inertia I of the rotating elements, and the wheel radius R . Also, g is the gravitational constant, γ is the rolling resistance coefficient, η is the air drag constant [3].

Using the simulation platform shown in Fig. 3 and the position and speed data s_1, v_1, \dots, v_n during each experiment, we are able to obtain the fuel consumption m_f of the connected automated truck for different gain combinations. In this way, we are able to find the gains that minimize fuel consumption.

V. DESIGN RESULTS

In this section, we consider the driving scenario shown in Fig. 2(a), and apply the optimization methods in Section IV to obtain desirable parameter values for the connected automated truck.

We set the speed limit $v_{\text{max}} = 35$ [m/s], stopping distance $h_{\text{st},0} = 5$ [m], and gradient $\kappa_0 = 0.6$ [1/s] for the range policy function of the connected automated truck. We fix the feedback gain $\alpha = 0.4$ [1/s] so that the truck could maintain a safe distance from its immediate predecessor. For the sake of simplicity, we only consider connectivity with three vehicles ahead, that is, the energy efficiency/fuel consumption will be optimized over the design space of $\mathbf{p}_3 = [\beta_1, \beta_2, \beta_3]$.

When computing the level sets of the objective function (14), we use the amplitude spectra shown in Fig. 1(d). For all human-driven vehicles, we set $\alpha_{h,i} = 0.2$ [1/s], $\beta_{h,i} = 0.4$ [1/s], $\kappa_i = 0.6$ [1/s], $\tau_i = 0.9$ [s] based on experimental data [7]. For the connected automated truck, we set the lumped delay $\sigma = 0.7$ [s]; cf. (8).

When minimizing the fuel consumption using TruckSim simulation, we set the information delay $\xi_i = 0.1$ [s] in the higher-level connected cruise controller (5), which corresponds to the V2V communication frequency of 10 [Hz]. For the saturation function $\text{sat}_0(\cdot)$ of the connected automated truck, we set $u_{\text{max},0} = 1$ [m/s²] and $u_{\text{min},0} = -4$ [m/s²].

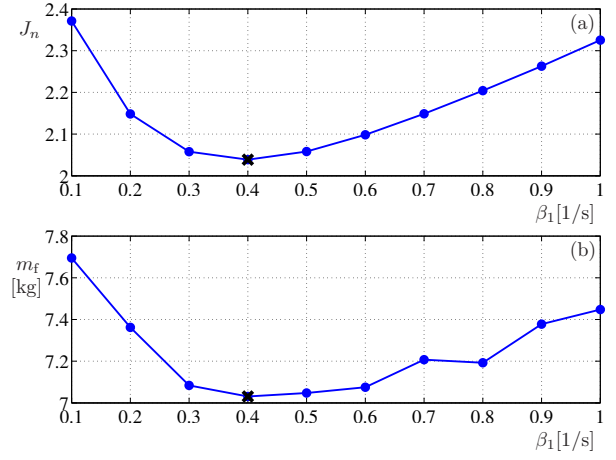


Fig. 4: (a) The value of objective function (14) as a function of β_1 . (b) The total mass of fuel m_f consumed by the truck in the high-fidelity simulation as a function of β_1 .

A. Benchmark: only using information from one vehicle

To establish a benchmark for the proposed connected cruise controller, we first consider the case when the truck only uses motion information from vehicle immediately ahead, that is, $n = 1$ in (5) and β_1 is the only design parameter.

For the energy efficiency evaluation, we use the amplitude spectrum $\rho_1(\omega)$ (shown in red in Fig. 1(d)) in the objective function (14). We plot the value of (14) as a function of β_1 in Fig. 4(a) with step size 0.1 [1/s]. The minimum is marked by the black cross at $\beta_1 = 0.4$ [1/s]. For the fuel consumption optimization, we load the motion data of vehicle 1 (cf. Fig. 1) into the TruckSim platform, and we plot the total mass of fuel m_f consumed by the connected automated truck in Fig. 4(b) with the same step size. Note that the curves in Fig. 4(a,b) are qualitatively similar. In particular, the optimal design parameter is $\beta_1 = 0.4$ [1/s] for both cases. Thus, we pick $[\beta_1, \beta_2, \beta_3] = [0.4, 0, 0]$ [1/s] as the benchmark.

B. Exploiting motion information from multiple vehicles

We now utilize motion information from vehicles 1, 2, 3 in the connected cruise controller (5). Using the speed data and amplitude spectrum shown in Fig. 1, we compute the energy efficiency (14) and fuel consumption m_f for different $[\beta_1, \beta_2, \beta_3]$ combinations (with 0.1 [1/s] resolution).

As an example, in Fig. 5(a), we show the level sets of the energy efficiency (14) in the (β_2, β_3) -plane for $\beta_1 = 0.1$ [1/s]. The minimum value is achieved at $\mathbf{p}_n^* = [\beta_1^*, \beta_2^*, \beta_3^*] = [0.1, 0.4, 0.4]$ [1/s], as marked by the black cross in Fig. 5(a). Note that not only the minimum value $J_n(\mathbf{p}_n^*) = 0.79$ is significantly smaller than the minimum in Fig. 4(a), but most contours in Fig. 5(a) indicate better energy efficiency than the minimum in Fig. 4(a). This shows the significant benefits of including the speed data from vehicles farther ahead.

In Fig. 5(b) we show the level sets of m_f in the (β_1, β_2) -plane for $\beta_3 = 0.1$ [1/s]. The fuel-optimal parameter combination is $[\beta_1, \beta_2, \beta_3] = [0.1, 0.2, 0.7]$ [1/s], as marked by the

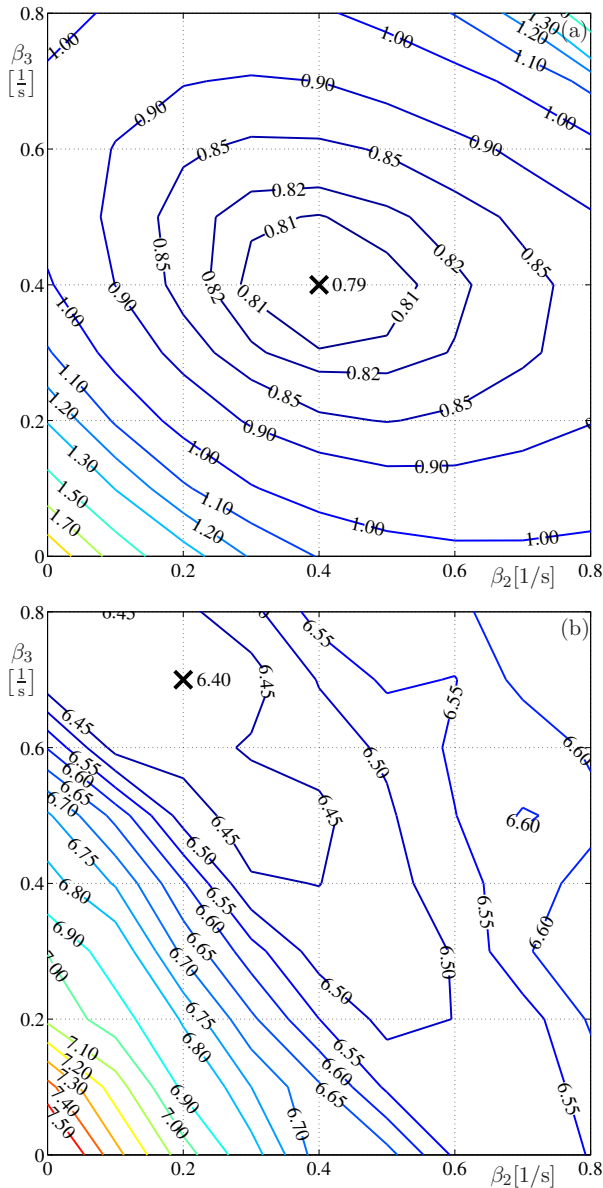


Fig. 5: (a) The level sets of objective function (14) in the (β_2, β_3) -plane for $\beta_1 = 0.1$ [1/s]. (b) The level sets of the fuel consumption m_f in the (β_2, β_3) -plane for $\beta_1 = 0.1$ [1/s]. The black crosses denote the location of the minima.

black cross in Fig. 5(b). This is fairly close to the energy-optimal parameters (black cross in Fig. 5(a)). Again most level sets in Fig. 5(b) show less fuel consumption than the minimum in Fig. 4(b). This indicates that even with nonlinearities in the powertrain and vehicle dynamics, adding feedback terms from vehicles farther ahead can be beneficial for fuel economy.

To further demonstrate the benefits of utilizing motion information from vehicles farther ahead, we plot the time profiles corresponding to the fuel-optimal parameters $[\beta_1, \beta_2, \beta_3] = [0.1, 0.2, 0.7]$ [1/s] in red, the energy-optimal parameters $[\beta_1, \beta_2, \beta_3] = [0.1, 0.4, 0.4]$ [1/s] in dashed green, and the benchmark parameters $[\beta_1, \beta_2, \beta_3] = [0.4, 0, 0]$ [1/s] in blue in Fig. 6. In Fig. 6(a,b), the connected automated

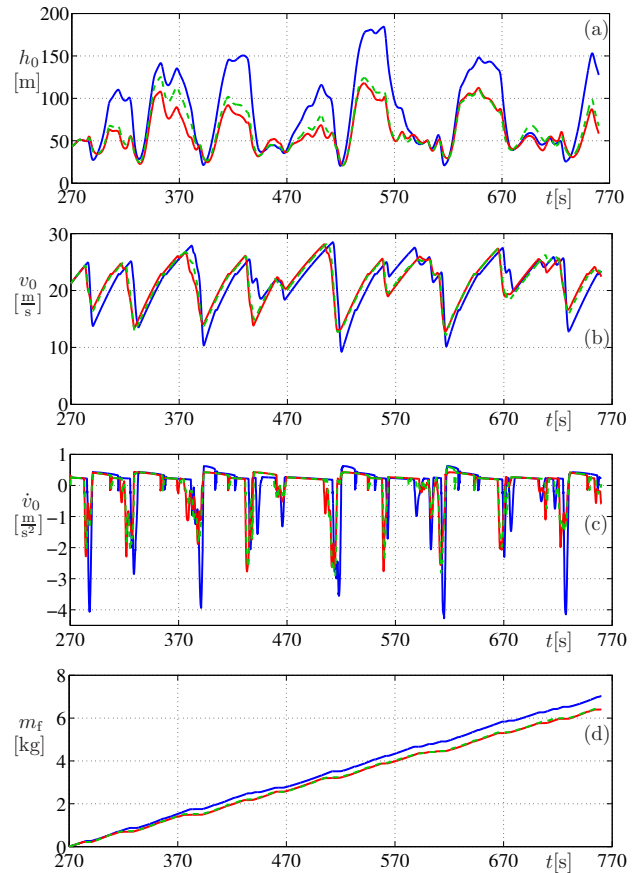


Fig. 6: Simulation results with different gain combinations. (a) Time profiles of the connected automated truck's headway h_0 . The red and green dashed curve corresponds to the fuel-optimal design when motion information from vehicles 1, 2, 3 are utilized, with red curve using $[\beta_1, \beta_2, \beta_3] = [0.1, 0.2, 0.7]$ [1/s] while green dashed curve using $[\beta_1, \beta_2, \beta_3] = [0.1, 0.4, 0.4]$ [1/s]. The blue curve corresponds to the benchmark design when motion information only from vehicle 1 is used ($[\beta_1, \beta_2, \beta_3] = [0.4, 0, 0]$ [1/s]). (b) Time profiles of the velocity v_0 . (c) Time profiles of the acceleration \dot{v}_0 . (d) The mass of fuel m_f consumed by the connected automated truck as a function of time.

truck shows significantly smaller headway and speed fluctuations when using the fuel-optimal parameters (red) or energy-optimal parameters (dashed green) compared with the benchmark parameters (blue). In Fig. 6(d), at the end of the simulation, the both fuel-optimal and energy-optimal design consumes about 8% less fuel compared with the benchmark design. Fig. 6(c) highlights the reason behind this significant improvement: the energy-efficient and fuel-efficient designs accelerate/brake earlier and milder than the benchmark design. With less energy dissipated in braking, the connected automated truck requests less energy from the engine and consumes less fuel.

VI. ROBUSTNESS OF FUEL-OPTIMAL CONNECTED CRUISE CONTROL DESIGN

In the previous sections, we obtained the benchmark gains for a connected automated truck using only motion information from the vehicle immediately ahead, and energy-optimal

and fuel-optimal gains when utilizing motion information from three vehicles ahead. These gains are obtained by using the speed data collected during one experiment (referred to as Set 1 here). However, it is important that given similar speed profiles on road, the energy/fuel-optimal gains maintain their benefits over the benchmark gains. Such robustness against variations in traffic data is crucial for the implementation of connected automated trucks in real traffic. In this section, we evaluate the fuel consumption of the connected automated truck in TruckSim in six different data sets, and examine the performance of the benchmark, energy-optimal, and fuel-optimal gains determined above.

In Table I, we show the fuel consumption m_f at the end of the runs, maximum headway \bar{h} , and minimum headway \underline{h} for each data set. Recall that Set 1 was used in finding the benchmark, energy-optimal, and fuel-optimal gains. In this case the benchmark gains consume the most amount of fuel, while the energy-optimal gains provide 8.3% improvement and the fuel-optimal gains provide 9.0% improvement. Also, the energy-optimal and fuel-optimal gains have smaller maximum headway \bar{h} and larger minimum headway \underline{h} compared with the benchmark case, indicating that better fuel economy is achieved without sacrificing safety or traffic efficiency. For Sets 2, . . . , 6, the energy-optimal and fuel-optimal gains still produce 4-13% improvement in fuel economy compared with the benchmark case, while their headway fluctuations are still smaller. These results demonstrate that the connected cruise controller designed under a particular data set can be used for similar data sets to maintain high energy efficiency and low fuel consumption.

VII. CONCLUSION

In this paper, we proposed a data-based method to optimize the energy efficiency and minimize the fuel consumption of connected automated trucks. We collected speed profiles of human-driven vehicles on road and obtained their Fourier spectra. Then we proposed an analytical method to quantify the energy efficiency of connected cruise controllers by utilizing the head-to-tail transfer function. We also established a high-fidelity simulation platform to minimize the fuel consumption using experimental data and showed that the energy-optimal is close to the fuel-optimal one. We found that utilizing motion information from multiple vehicles ahead may improve both safety and fuel economy of connected automated trucks, and such improvements are robust against variations in traffic data.

ACKNOWLEDGEMENT

The authors would like to thank Navistar, Inc. and Comm-signia, Inc. for their technical support, and acknowledge the help of Sándor Beregi, Zsuzsanna Dobránszky, Ádám Kiss, and Henrik Sykora during the experiments.

REFERENCES

[1] U.S. Department of Transportation, “Commodity Flow Survey: United States: 2012,” Tech. Rep., 2015.

Set	β_1	β_2	β_3	$m_f(t_f)$ [kg]	Percent	\bar{h} [m]	\underline{h} [m]
1	0.4	0	0	7.03	—	184	20
1	0.1	0.4	0.4	6.45	8.3%	125	21
1	0.1	0.2	0.7	6.40	9.0%	118	21
2	0.4	0	0	7.35	—	279	23
2	0.1	0.4	0.4	6.96	5.3%	216	26
2	0.1	0.2	0.7	7.05	4.2%	193	27
3	0.4	0	0	7.93	—	205	11
3	0.1	0.4	0.4	6.98	11.9%	180	12
3	0.1	0.2	0.7	6.87	13.4%	171	12
4	0.4	0	0	8.13	—	218	12
4	0.1	0.4	0.4	7.24	11.0%	190	12
4	0.1	0.2	0.7	7.22	11.2%	190	12
5	0.4	0	0	8.07	—	241	19
5	0.1	0.4	0.4	7.21	10.7%	202	12
5	0.1	0.2	0.7	7.26	10.1%	190	11
6	0.4	0	0	8.37	—	342	5
6	0.1	0.4	0.4	7.80	6.8%	309	5
6	0.1	0.2	0.7	7.74	7.4%	302	5

TABLE I: Performance of the connected automated truck using the benchmark gains $[\beta_1, \beta_2, \beta_3]=[0.4, 0, 0]$ [1/s], the energy-optimal gains $[\beta_1, \beta_2, \beta_3]=[0.1, 0.4, 0.4]$ [1/s] and the fuel-optimal gains $[\beta_1, \beta_2, \beta_3]=[0.1, 0.2, 0.7]$ [1/s] under different traffic datasets. The fuel-economy performance is represented by the mass of consumed fuel m_f at the end of the run, and the percentage of improvement with respect to the benchmark case. The headway performance is shown by the maximum headway \bar{h} and minimum headway \underline{h} .

[2] A. Sciarretta, G. De Nunzio, and L. Ojeda, “Optimal ecodriving control: Energy-efficient driving of road vehicles as an optimal control problem,” *IEEE Control Systems Magazine*, vol. 35, no. 5, pp. 71–90, 2015.

[3] C. R. He, H. Maurer, and G. Orosz, “Fuel consumption optimization of heavy-duty vehicles with grade, wind, and traffic information,” *Journal of Computational and Nonlinear Dynamics*, vol. 11, no. 6, p. 061011, 2016.

[4] X.-Y. Lu and S. Shladover, “Integrated ACC and CACC development for heavy-duty truck partial automation,” in *Proceeding of 2017 American Control Conference*, May 2017, pp. 4938–4945.

[5] V. Turri, B. Besselink, and K. H. Johansson, “Cooperative look-ahead control for fuel-efficient and safe heavy-duty vehicle platooning,” *IEEE Transactions on Control Systems Technology*, vol. 25, no. 1, pp. 12–28, Jan 2017.

[6] G. Orosz, “Connected cruise control: modelling, delay effects, and nonlinear behaviour,” *Vehicle System Dynamics*, vol. 54, no. 8, pp. 1147–1176, 2016.

[7] J. I. Ge and G. Orosz, “Connected cruise control among human-driver vehicles: experiment based parameter estimation and optimal control design,” *Transportation Research Part C*, p. under review, 2017.

[8] J. I. Ge, S. S. Avedisov, C. R. He, W. B. Qin, M. Sadeghpour, and G. Orosz, “Experimental validation of connected automated vehicle design among human-driven vehicles – impacts on traffic safety and efficiency,” *Transportation Research Part C*, p. under review, 2017.

[9] I. V. Kolmanovsky and D. Filev, “Terrain and traffic optimized vehicle speed control,” in *Advances in Automotive Control*, 2010, pp. 378–383.

[10] S. E. Li, Q. Guo, S. Xu, J. Duan, S. Li, C. Li, and K. Su, “Performance enhanced predictive control for adaptive cruise control system considering road elevation information,” *IEEE Transactions on Intelligent Vehicles*, vol. 2, no. 3, pp. 150–160, 2017.

[11] C. R. He and G. Orosz, “Saving fuel using wireless vehicle-to-vehicle communication,” in *Proceeding of 2017 American Control Conference*, 2017, pp. 4946–4951.

[12] B. S. Kerner, *The Physics of Traffic: Empirical Freeway Pattern Features, Engineering Applications, and Theory*. Springer, 2012.

[13] L. Zhang and G. Orosz, “Motif-based design for connected vehicle systems in presence of heterogeneous connectivity structures and time delays,” *IEEE Transactions on Intelligent Transportation Systems*, vol. 17, no. 6, pp. 1638–1651, June 2016.

[14] Navistar, “Maxxforce 11 and 13 liter engines,” Navistar Inc., Tech. Rep., 2011.